

Aharonov-Bohm and quantum Hall effects in singly connected quantum dots

U. Sivan

Raymond and Beverly Sackler Faculty of Exact Sciences, School of Physics and Astronomy, Tel Aviv University, 69 978 Tel Aviv, Israel

Y. Imry

Department of Nuclear Physics, Weizmann Institute of Science, 76 100 Rehovot, Israel

C. Hartzstein

Raymond and Beverly Sackler Faculty of Exact Sciences, School of Physics and Astronomy, Tel Aviv University, 69 978 Tel Aviv, Israel

(Received 17 June 1988)

The magnetotransport due to edge states in a two-dimensional (2D) system smaller than the appropriate phase coherence length is considered. For a 2D “quantum dot” driven by two narrower leads and a Fermi energy in the edge-states regime, we find Aharonov-Bohm-type oscillations in both the longitudinal and the Hall conductances. The latter oscillations are superimposed on the quantized value (e^2/h) for single-channel leads. The oscillations survive a substantial amount of disorder. Next, the strip geometry is examined and conditions for Hall quantization are formulated. These conditions are far less restrictive than previously published ones.

I. INTRODUCTION

Surface states in strong magnetic fields¹⁻⁴ and the currents associated with them are known to have significant effects on both thermodynamic [e.g., the Landau diamagnetism and the de Haas-van Alphen (dHvA) oscillations] and transport [including the Shubnikov-de Haas and the quantum Hall (QHE) effects] properties. In the semiclassical picture²⁻⁵ these states correspond to the “whispering gallery” trajectories, grazing the sample’s boundary. In some geometries (e.g., a disk) this results in an effective ring topology which may lead, in analogy with experiments in superconducting and normal rings,⁶ to an Aharonov-Bohm (AB) type of oscillations in *singly connected samples*. In fact, such oscillations in the weak-field limit and for extremely pure samples were predicted by Bogachek and Gogadze⁷ (thermodynamic quantities) and by Peschanskii and Sinolitskii⁸ (magnetoresistance). They were later demonstrated in a series of beautiful experiments in pure, single-crystal bismuth cylinders by Brandt *et al.*⁹ Recently, Sivan and Imry¹⁰ have shown such oscillations in the magnetization of a finite disk, shorter than the phase coherence length in a strong-field limit (QHE regime). In particular it was demonstrated that these oscillations survive a rather strong disorder (comparable to $\hbar\omega_c$) and that their period corresponds indeed to approximately one flux quantum threading the whole sample. The purpose of the present paper is to deal with a similar AB type of oscillations in transport phenomena and in particular in the extremely interesting “quantized” Hall conductance.¹¹⁻¹⁴

In Sec. II we present the model to be studied numerically (consisting of a 2D square fed by two ideal single-channel leads connected to its vertices) and explain the method employed in the calculations. Section III is devoted to the spectrum of an isolated “quantum dot” and in particular to the edge states. A simplified “ring” mod-

el for the transport, predicting many of the numerical results, is presented in Sec. IV. The conductance is obtained in a Landauer-type picture¹⁵ while the Hall conductance is calculated using a formula given by Entin-Wohlman *et al.*¹⁶ The results of the numerical calculations, including disorder, are given in Sec. V for the longitudinal resistance and in Sec. VI for the Hall resistance. A particularly interesting result is an AB oscillation superimposed on the QHE. Finally, in Sec. VII we discuss the Landauer multichannel strip model, suggested recently by Streda *et al.*¹² Their sum rule is corrected, an interesting asymmetry is pointed out, and conditions for the QHE are formulated, including its general existence in the case of single-channel edge states—in agreement with the results in Sec. VI.

II. THE MODEL

The model considered (Fig. 1) consists of a 2D square of $L \times L = N$ sites, fed by two semi-infinite 1D perfect leads.¹⁶ A tight-binding Hamiltonian with diagonal disorder (Anderson model) is assumed:

$$H = \sum_i \epsilon_i |i\rangle \langle i| + \sum_{i,j} V_{ij} |i\rangle \langle j| ,$$

where the ϵ_i are zero on the leads and distributed randomly in an interval $[-W, W]$ on the square. The coupling constants V_{ij} in the leads are V for nearest neighbors and zero elsewhere. For a magnetic field pointing out of the page, in the Landau gauge $\mathbf{A} = (-yB, 0, 0)$, the nearest-neighbor coupling constants in the square take the form $V_{k,j} = \exp[2\pi i(x_j - x_k)y_k \phi / \phi_0]$ (in all numerical results presented later, we set $V=2$ to guarantee equal bandwidths in the leads and in the square). The disorder is restricted to the square alone (excluding the vertices). The effect of the magnetic field on the atomic orbitals is neglected.

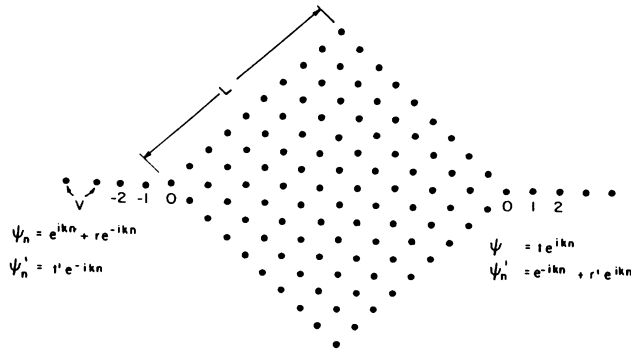


FIG. 1. The tight-binding model studied numerically. A $2D$ square of $L \times L$ sites, fed by two semi-infinite $1D$ perfect leads.

Determination of the chemical potential on a given site involves two scattering experiments,¹⁶ from the left-hand side and the right-hand side. A scattering state on the left-hand side (LHS) lead, for a particle impinging from the LHS, is $\psi_n = \exp(ikn) + r \exp(-ikn)$, $n=0, -1, -2, \dots$, where r is the reflection amplitude and k is the longitudinal k vector satisfying the dispersion relation $E = 2V \cos(ka)$ (a being the lattice constant). A scattering state on the right-hand side (RHS) for a particle impinging from the LHS is given by $\psi_n = t \exp(ikn)$, $n=0, 1, 2, \dots$. Similarly, for a particle impinging from the RHS, the scattering amplitudes on the LHS and RHS are $\psi'_n = t' \exp(-ikn)$ and $\psi'_n = \exp(-ikn) + r' \exp(ikn)$, respectively. $t, t', r,$ and r' are related by $t = t'$ and $t/r = -t^*/r^*$. Substituting t and $1+r$ for the wave-function amplitudes on the opposite corners, it is possible to eliminate the $1D$ leads from the Hamiltonian and obtain the following equation for the wave-function amplitudes:

$$(H' - E)\Psi = C, \quad (1)$$

with $H'_{ij} = H_{ij} - (\delta_{i,1}\delta_{j,1} + \delta_{i,N}\delta_{j,N})V \exp(-ika)$, H being the Hamiltonian of an isolated square. C is different for left and right scattering. For the former, $C_1 = V \exp(ika)$, $C_2 = V_{L,1}$, $C_{L+1} = -1$, and $C_i = 0$ for $i \neq 1, 2, L+1$. For the latter case, the nonvanishing elements are $C'_{N-L-1} = C'_{N-1} = -1$ and $C'_N = V$. The transmission (t) and reflection (r) coefficients are then given by ψ_N and ψ_1 , respectively. Similarly, t' and r' are given by ψ'_1 and ψ'_N . Notice that the wave-function amplitudes in the different sites are not normalized.

III. SPECTRUM OF A "QUANTUM DOT"

The spectrum of an almost ordered ($W=0.01$) isolated 10×10 square, in the tight-binding model is shown in Fig. 2 as a function of ϕ/ϕ_0 (see also Ref. 17). The energy is measured in units of V . The various zones, $A, B, C,$ and D , correspond to four different regimes.

A. Weak-field regime (Refs. 2–4 and 7–9)

The cyclotron radius is large compared with the linear dimensions of the sample and the quantization is mainly due to finite sample size. For the n th Landau level this

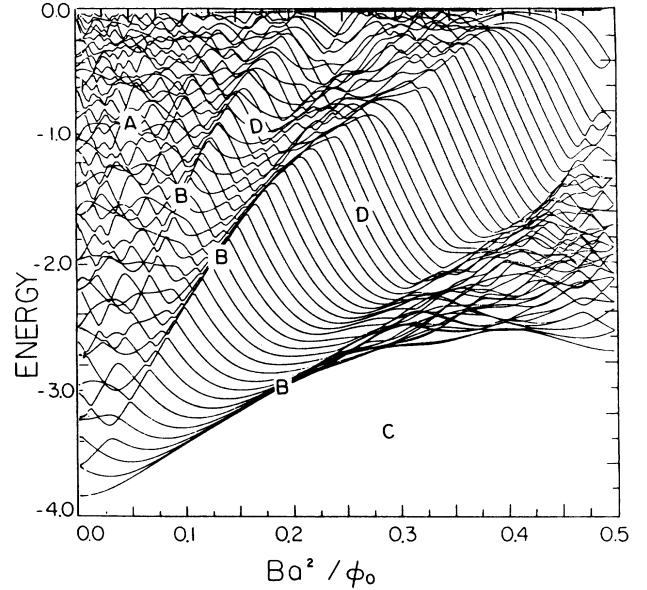


FIG. 2. The lowest 50 levels of a 10×10 tight-binding Anderson model as functions of the flux through a unit cell, in units of ϕ_0 . The absolute value of the nearest-neighbor matrix element is unity and $W=0.01$. $A, B, C,$ and D correspond to the different regimes (see text).

implies $L_H^n > L$, where $L_H^n = \sqrt{2n+1}L_H$ and $L_H = \sqrt{\hbar c/eB}$ is the magnetic length.

B. Bulk Landau levels

The n th Landau level forms for L_H^n smaller than L . The semiclassical trajectories pertaining to these states are limited to the bulk and do not intersect with the boundaries. For not too strong magnetic fields, their energies are given in the effective-mass approximation (up to small finite size modification) by $M = \hbar^2/2V$, $\hbar\omega_c = 4\pi V\phi/\phi_0$, and $E_{n,m} = \hbar\omega_c(n + \frac{1}{2})$. At stronger magnetic fields, when L_H is not much larger than a , this behavior changes dramatically and becomes very complicated.¹⁸

C. Magnetic barrier

For energies lower than the first Landau level, the density of states vanishes. Later on we show that if the Fermi energy is set to that region, the transmittance of the sample depicted in Fig. 1 is exponentially small.

D. Edge states (Refs. 1–4 and 7–14)

This regime is the main subject of the present work. Surface (or edge, in the $2D$ case discussed here) states correspond to the quasiclassical "whispering gallery" states,^{2–4} that is, eigenfunctions whose semiclassical trajectories are confined to the vicinity of the edges. For $n \sim 1$ these states appear for $L_H \leq L$ and consist of a fraction L_H/L of the total number of states. Their energies reside in the gaps between Landau levels and the average

energy spacing between consecutive edge states, in the same Landau level, is of the order of $\hbar\omega_c L_H/L$. The classical motion of the guiding center is in the opposite direction to that of the cyclotron motion, which has been argued to lead classically to exact cancellation of the bulk magnetization by the surface states.¹ In Fig. 2, it manifests itself in the negative slope of the energy as a function of flux (orbital magnetism parallel to the magnetic field). The probability distributions $|\psi(n)|^2$ for typical scattering surface states (from the LHS, and therefore concentrated along the upper edge of the sample) at two degrees of disorder ($W=0$ and 2) are exhibited in Figs. 3(a) and 3(b), respectively. Indeed, the probability to find the particle is significantly higher near the edges and especially near the upper one. The edge states of an ordered infinite strip,¹³ propagating from left to right, are confined to the upper edge. The finite probability to find the particle near the lower edge is due to scattering from the upper channels to the lower ones caused by the special geometry in Fig. 1 and by the disorder [compare Figs. 3(a) and 3(b)]. Since these states exist near the edges, small changes in the magnetic flux affect them like an Aharonov-Bohm flux through a ring,^{19,20} leading to approximately periodic oscillations of both thermodynamic¹⁰ and transport properties. This is the essence of the magnetoconductance oscillations demonstrated in the next section and the oscillations in the Hall conductance discussed in Sec. V.

Edge states (and hence the AB oscillations considered) survive a substantial amount of disorder^{10,11} (up to $W \sim \hbar\omega_c$ in our model¹⁰). This robustness is due to the separation in both space and energy between them and the bulk Landau levels. It follows also from the semiclassical, strong-field approximation, where the guiding center travels along equipotential lines.²¹⁻²³ In that picture, it takes bulk impurities with energies of the order of $\hbar\omega_c$ to create a percolating equipotential line connecting the upper edge to the lower one.

It is instructive to follow the path of a given occupied state in Fig. 2 as a function of flux. For very strong magnetic fields, the lowest Landau level accommodates all electrons. Upon reducing the magnetic field the degeneracy of that level decreases and one occupied state at a time becomes a surface state. Its energy increases as the flux is

reduced until it becomes finally degenerate with the next Landau level and that electron starts to populate the latter level. A further decrease in the flux results in the usual, bulk energy level decrease until the decreasing degeneracy of that Landau level can no longer accommodate all electrons and it becomes again a surface electron. The smooth transition between bulk levels through surface states smears the sharp bulk oscillations¹⁰ in the magnetization (de Haas-van Alphen) and in the magnetoconductance (Shubnikov-de Hass).

IV. A MODEL FOR TRANSPORT VIA EDGE STATES

For $W \ll \hbar\omega_c$ and a Fermi energy in the gap between bulk Landau levels, the transport through the system depicted in Fig. 1 can be modeled by the 1D ring²⁴ depicted in Fig. 4. The ring is driven by two particle reservoirs of chemical potentials μ_1 and μ_2 , connected by two infinite, perfect 1D leads. For \mathbf{B} pointing out of the page and negatively charged carriers, the states propagating from left to right pass through the upper arm of the ring while those propagating in the opposite direction follow the lower arm. For the sake of simplicity it is assumed that all scattering (due to geometry and disorder) occurs in the junctions. This assumption is motivated by the small spatial overlap between rightward and leftward-propagating states, except for the vicinity of the corners (Figs. 3). For stronger disorder ($W \geq \hbar\omega_c$), edge states on opposite corners are coupled via bulk states and the model considered is no longer valid.

For a particle impinging from the LHS we denote the wave functions amplitudes in the upper and lower arms, right after the LHS junction, by $u_{l,1}$ and $d_{l,1}$ respectively. $u_{l,2}$ and $d_{l,2}$ are the corresponding amplitudes in the vicinity of the RHS junction,

$$u_{l,2} = u_{l,1} \exp(i\theta),$$

$$d_{l,2} = d_{l,1} \exp(-i\theta), \quad \theta = \pi\phi/\phi_0 + kL.$$

ϕ is the magnetic flux threading the ring and kL is the phase acquired by the partial wave traveling along the ring's arm in the absence of magnetic field.

The total transfer matrix for a particle impinging from

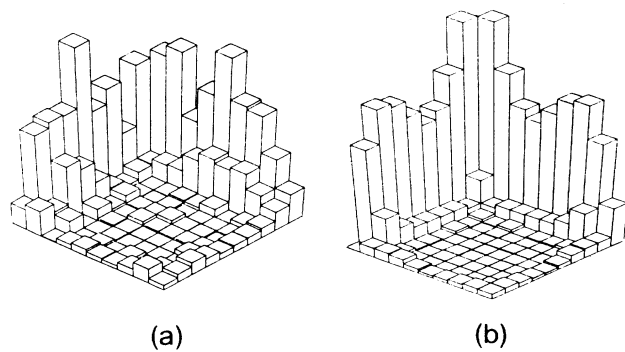


FIG. 3. The probability distribution $|\psi(r)|^2$ for typical surface states. $E = -2$ and (a) $W=0$, (b) $W=2$.

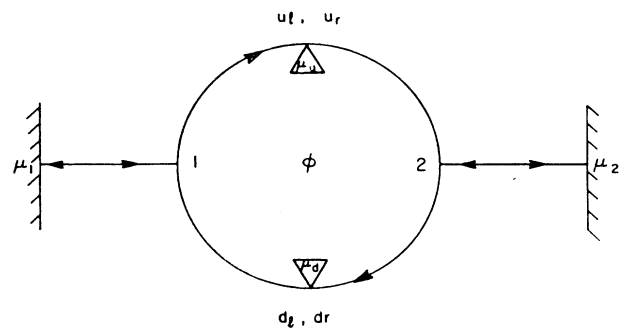


FIG. 4. A single-channel model for transport via edge states in the QHE regime. Contrary to real rings, the current circulates in one direction only.

the LHS is $\tau_2 \Theta \tau_1$ where τ_2 (τ_1) is the transfer matrix of the RHS (LHS) junction and $\Theta_{ij} = \delta_{i1} \delta_{j1} \exp(i\theta) + \delta_{i2} \delta_{j2} \exp(-i\theta)$. It then follows that the total transmission is given by

$$T = \frac{T_1 T_2}{1 + R_1 R_2 - 2 \operatorname{Re}[\exp(2i\theta) r_2 r_1']}, \quad (2)$$

where r_1' denotes the reflection amplitude of the LHS junction for a particle impinging from the RHS. In the derivation of Eq. (2) we have employed the relation $-t^*/t = r^*/r'$. The total current, being proportional to T , oscillates periodically as a function of ϕ with an amplitude given by $4(R_1 R_2)^{1/2} T_1 T_2 / (1 - R_1 R_2)^2$. Notice that within our model, for $R_1 = R_2$, there is always some value of ϕ (resonance condition) for which $T = 1$.

The Hall voltage is evaluated using Eq. (5) in Ref. 16 [Eq. (3) below]. Let us briefly rederive this result. To define the chemical potential on the upper arm we connect it to a measurement reservoir^{25,26} with a density of states n_r , chemical potential μ_u , and small coupling matrix elements squared $\epsilon|u_l|^2$ and $\epsilon|u_r|^2$ to the states coming from the outer LHS and RHS reservoirs, respectively (the wave functions of those states in the measurement region on the upper arm are denoted by u_l and u_r). Assuming $\mu_2 < \mu_u < \mu_1$, each full, rightward-propagating measurement reservoir state between μ_2 and μ_u can decay into the empty right-going states in the upper arm (originated in the RHS reservoir), with a rate, given by the golden rule, of $\epsilon|u_r|^2 n_0$, where n_0 is the density of the rightward-propagating states in the upper arm. Multiplying this rate by the number of such reservoir states, $n_r(\mu_u - \mu_2)$, gives the current from the reservoir to the upper arm. Similarly, the current from the full states in the upper arm into the reservoir is given by the rate $\epsilon|u_l|^2 n_r$ multiplied by the number of such states, $n_0(\mu_1 - \mu_u)$. The condition for zero net current between the upper arm and the measurement reservoir is obtained by equating these two currents and yields

$$\mu_u = \frac{\mu_1 |u_l|^2 + \mu_2 |u_r|^2}{|u_l|^2 + |u_r|^2}.$$

Likewise, one can define μ_d and obtain an analogous expression with u interchanged with d . Subtracting these expressions one obtains Eq. (5) in Ref. 16:

$$\mu_u - \mu_d = (\mu_1 - \mu_2) \frac{|u_l|^2 |d_r|^2 - |u_r|^2 |d_l|^2}{(|u_r|^2 + |u_l|^2)(|d_r|^2 + |d_l|^2)}. \quad (3)$$

The various amplitudes squared are given by

$$|u_l|^2 = \frac{T}{T_2}, \quad |d_l|^2 = T \frac{R_2}{T_2}, \quad |u_r|^2 = T \frac{R_1}{T_1}, \quad |d_r|^2 = \frac{T}{T_1},$$

where R_1, R_2, T_1, T_2 , are the reflection and transmission coefficients of the two junctions. Substituting these results into Eq. (3), the Hall voltage takes the form

$$eV_H = \mu_u - \mu_d = (\mu_1 - \mu_2) \frac{T_1 T_2}{1 - R_1 R_2}, \quad (4)$$

leading to the Hall conductivity

$$G_H = \frac{1 - R_1 R_2}{1 + R_1 R_2 - 2 \operatorname{Re}[\exp(2i\theta) r_2 r_1']} \frac{e^2}{h}. \quad (5)$$

Notice that the Hall voltage is independent of the flux.

The Hall conductivity oscillates periodically as a function of the flux threading the ring with an amplitude given by $4[(R_1 R_2)/(1 - R_1 R_2)]^{1/2} e^2/h$. Assuming $R_1 = R_2$ and using $\langle T \rangle = T_1 T_2 / (1 - R_1 R_2)$, the oscillation amplitude is given by

$$\Delta G_H = \frac{2(1 - \langle T \rangle)}{\sqrt{\langle T \rangle}} \frac{e^2}{h}. \quad (6)$$

Averaging Eq. (5) with respect to ϕ , one obtains the quantum Hall effect

$$\langle G_H \rangle = e^2/h.$$

Contrary to the condition cited in Ref. 12, the above result holds for $R \neq 0$ as well (see discussion in Sec. VII).

V. AB OSCILLATIONS IN THE MAGNETOCONDUCTANCE— NUMERICAL STUDY

The transmission coefficient $T = |t|^2$ versus ϕ/ϕ_0 for $E = -2$ and different two degrees of disorder is exhibited in Fig. 5. The arrows indicate the flux values corresponding to $E = -2$ in the spectrum of an ordered isolated square (Fig. 2). Notice, however, that the spectrum of the system under consideration (Fig. 1) is continuous due to the infinite 1D leads.

Tuning the flux between $0.1\phi_0$ and $0.5\phi_0$ we scan the second Landau level ($n = 1$), the surface states in the gap between the bulk levels, and finally the lowest Landau level. For a Fermi energy within the bulk Landau levels, the transmission coefficient T fluctuates rapidly as the

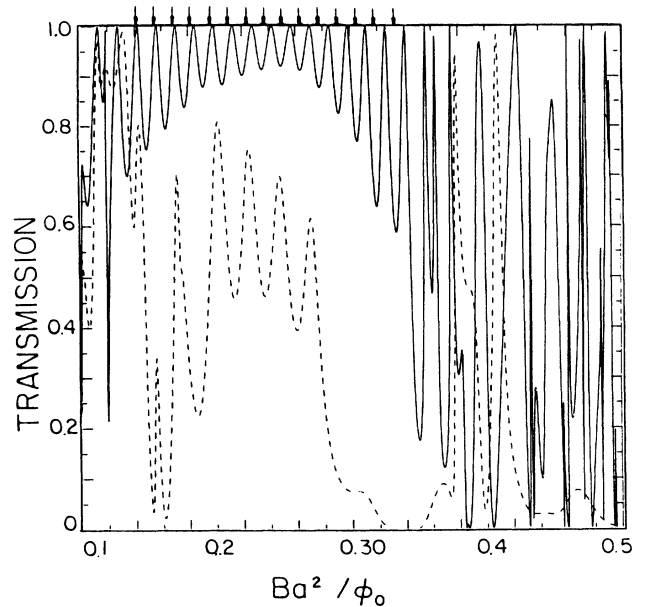


FIG. 5. The transmission coefficient T vs ϕ/ϕ_0 for the model depicted in Fig. 1. $E = -2$; the solid line corresponds to $W = 0$ and the dashed one to $W = 2$. The arrows indicate the flux values corresponding to $E = -2$ in the spectrum of an isolated square (Fig. 2).

flux through the whole sample is changed by fractions of ϕ_0 . The magnitude of these fluctuations, ΔT , is of the order of unity and they may be related to resonances. In the present work, however, we concentrate on edge states and we do not elaborate on the very interesting fluctuations due to bulk levels any further.

Upon increasing the magnetic field, the Fermi energy is shifted to the surface-states regime, in the gap between the two lowest Landau levels. The quasi-1D nature of these states, compared to the 2D normalization of bulk states, accounts for the relatively high transmission. The transmission oscillates with the flux, with a period depending on the disorder. In the ordered case, the period corresponds to an effective ring area of $\simeq 70 a^2$ while for $W=2$, the effective area shrinks to $\simeq 45 a^2$. This shrinkage can be qualitatively explained within the strong-field semiclassical approximation in which the guiding center follows equipotential lines. For $W=0$, the percolating equipotential lines, corresponding to edge states, pass along the edges. When the disorder is increased, the percolating equipotential contours are pushed to the bulk and the effective area shrinks. At even stronger disorder ($W > 2.5$, not shown here), the percolating contours no longer pass through the junctions with the leads and the AB oscillations disappear. The linkage between two conducting edge states by a bulk impurity and its contribution to magnetoconductance fluctuations observed in narrow wires were recently discussed in Ref. 27. The AB oscillations are due to interference between partial waves circulating the square different numbers of times. The small oscillation amplitude at $W=0$ is explained by the weak scattering from upper to lower states (see Figs. 3). Increasing the disorder we find that the oscillations are enhanced by stronger scattering to leftward-propagating

states, in agreement with the model developed in Sec. IV. We have found that as long as $W \ll \hbar\omega_c$, T reaches its maximal value (unity) periodically, which implies that most scattering take place in the corners [Eq. (2)]. The oscillations are extremely robust against static disorder and the perturbation energy W needed to smear them is of the order of $\hbar\omega_c$ (Sec. III). Similar oscillations occur when E_F is scanned in a fixed flux. Figure 6 depicts the transmission versus energy for $\phi=0.25\phi_0$ and two degrees of disorder, $W=0$ and $W=2$. The vanishing transmittance at the bottom of the band is due to the “magnetic barrier” corresponding to the vanishing density of states of an isolated square at energies lower than the lowest Landau level (Fig. 2, regime C). Notice that contrary to the stretching of the oscillations period, as a function of flux, when the disorder is increased, the period in energy is almost independent of W .

Although experimentally the shape considered here might not be realistic, we point out that similar effects may follow due to any abrupt change in the geometry²⁸ (e.g., a branch for Hall contacts) or imperfections.

VI. QHE AND AB OSCILLATIONS IN THE HALL CONDUCTIVITY — NUMERICAL STUDY

The dimensionless Hall conductance $g_H = T(\mu_1 - \mu_2) / (\mu_u - \mu_d)$ versus ϕ/ϕ_0 for $E = -2$ and two degrees of disorder ($W=0$ and $W=2$) is depicted in Fig. 7. Evaluation of the chemical potential at a given point involves the wave function’s amplitudes for LHS and RHS scattering experiments (see Sec. IV for detailed description of the calculation method). The chemical potential gradient $\mu_u - \mu_d$ needed for Fig. 7 was defined using Eq.

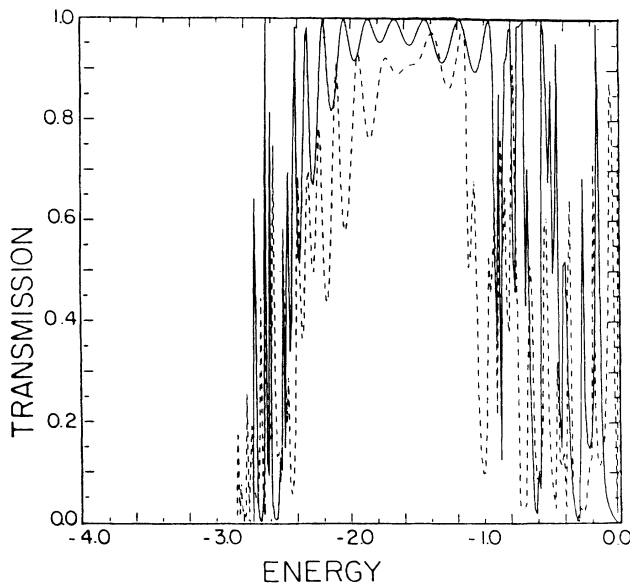


FIG. 6. The transmission coefficient T vs energy for $\phi/\phi_0=0.25$ and two degrees of disorder, $W=0$ (solid line) and $W=2$ (dashed line).

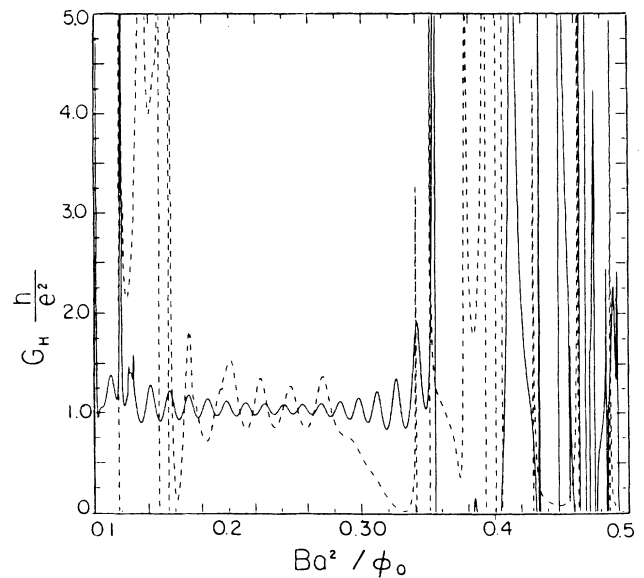


FIG. 7. The dimensionless Hall conductance vs ϕ/ϕ_0 for $E = -2$ and two degrees of disorder, $W=0$ (solid line) and $W=2$ (dashed line). Notice the AB oscillations superimposed on the quantized value.

(3) with u and d given by the averages of the wave function squared on the upper and lower edges, respectively (see Fig. 1). This definition is meant to simulate a measurement by two additional particle reservoirs, weakly coupled to the square's edges.^{25,26} It is by no means the only possible definition and a fuller discussion, including the effects of the reservoirs on the system, is given by Büttiker.²⁹

For a Fermi energy in the bulk Landau levels, g_H fluctuates rapidly with a huge amplitude (of the order of 10^2 – 10^3). Tuning the flux to the edge-states regime we observe periodic AB oscillations. In the model of Sec. IV, the Hall voltage was nonoscillatory [Eq. (4)] and, indeed, the voltage-oscillation amplitudes measured in the present geometry are very small. The oscillations in g_H are therefore attributed to current oscillations. The oscillations are enhanced for larger disorder and their amplitudes agree fairly well with Eq. (6). The period change was discussed in Sec. V.

The main and most important result demonstrated in Fig. 7 is the quantization of $\langle g_H \rangle$ predicted by our model (Sec. IV). Increasing W from 0 to 2, the longitudinal conductivity is reduced by more than an order of magnitude with almost no effect on $\langle g_H \rangle \simeq 1.05$ (we believe that the nonintegral value of $\langle g_H \rangle$ is probably due to the specific definition of $\mu_u - \mu_d$ we chose). We have also measured g_H for a Fermi energy in the surface-states regime, in the gap between the second ($n = 1$) and the third Landau level. Although accuracy was limited by the small size of our sample the results again indicate $\langle g_H \rangle \simeq 1$, compared to the $\langle g_H \rangle \simeq 2$ expected in the multichannel case (see Sec. VII below).

VII. THE MULTICHANNEL LANDAUER FORMULATION OF STREDA, KUCERA, AND MACDONALD AND THE RELATIONSHIP BETWEEN THE QHE AND THE "QUANTIZED CONTACT RESISTANCE"

Recently, Streda, Kucera and MacDonald¹² (SKM) formulated the strong-field transport due to edge states in a finite-width 2D system as a multichannel Landauer problem,^{26,30} depicted in Fig. 8. Two electron reservoirs of chemical potentials μ_1 and μ_2 ($\mu_1 \geq \mu_2$) are connected by ideal leads to the disordered region of the sample. The special feature of the model, for μ_1 and μ_2 lying in the

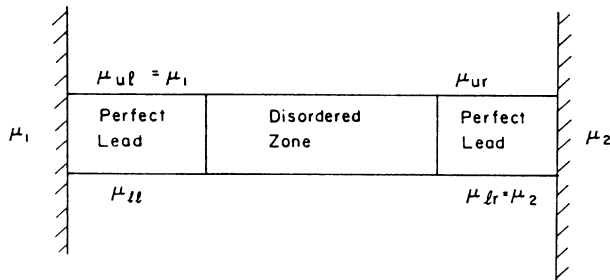


FIG. 8. The geometry considered by SKM. A finite strip driven by two particle reservoirs with chemical potentials $\mu_1 \geq \mu_2$.

gap between bulk Landau levels in the leads, is that the current-carrying edge states are localized on the upper (lower) edge for right- (left-) going currents (\mathbf{B} points out of the page and the carriers are negatively charged). The number of current-carrying channels in the leads is equal to the number, n , of occupied bulk Landau levels (or the integer n in the quantized Hall conductance ne^2/h , whenever conditions for the QHE hold). Thus, compared with the usual multichannel Landauer case, the channel number can be made of the order of unity by applying a strong enough magnetic field. The spatial separation of rightward- and leftward-propagating channels simplifies the problem considerably. Below, we briefly summarize the SKM formulation, our new observations and corrected physical consequences following from them. This includes the sum rule derived by SKM, conditions for the QHE to hold, and the important relationship with the quantized contact resistance.^{6,31,32}

The LHS reservoir is assumed to fill the n upper LHS edge states up to μ_1 , where their velocities are v_i . Likewise, the RHS reservoir feeds the n lower RHS states up to μ_2 . The transmission of the former states to upper-RHS states is given by an $n \times n$ matrix T_{ij} while their reflections into lower-LHS states are given by a matrix R_{ij} . The transmission and reflection coefficients of the lower-RHS states are likewise given by T'_{ij} and R'_{ij} , respectively (here, the definition of the matrices is similar to that in Ref. 30). The reflection and transmission matrices satisfy the unitarity conditions

$$\sum_j R_{ij} + T'_{ij} = 1, \quad \sum_j R'_{ij} + T_{ij} = 1, \quad (7)$$

$$\sum_i R_{ij} + T_{ij} = 1, \quad \sum_i R'_{ij} + T'_{ij} = 1, \quad (8)$$

and the time-reversal conditions

$$T_{ij}(H) = T'_{ji}(-H), \quad R_{ij}(H) = R_{ji}(-H), \quad (9)$$

$$R'_{ij}(H) = R'_{ji}(-H).$$

Let us define $T_i = \sum_j T_{ij}$ and $R_i = \sum_j R_{ij} = 1 - T'_i$. The current is then given by³⁰

$$I = \frac{e}{h} (\mu_1 - \mu_2) \sum_i T_i, \quad (10)$$

leading to the two-terminal conductance (with voltage measured between the driving reservoirs with chemical potentials μ_1 and μ_2)

$$G_0 = \frac{e^2}{h} \sum_i T_i. \quad (11)$$

In a case which will turn out later to be relevant for the QHE, where there are no reflections (no backscattering) and $R_{ij} = 0$, $R'_{ij} = 0$, it follows from Eqs. (7), (8), and (11) that

$$G_0 = n \frac{e^2}{h}. \quad (12)$$

The conductance quantization in the ordered case (for which the four-terminal resistance vanishes) was predicted by one of us.⁶ It may be attributed to contact resis-

tances in the connections of the wire to the reservoirs. Recently, this quantization was observed by van Wees *et al.*³¹ and Wharam *et al.*³² We emphasize that a relevant sufficient condition for that quantization is *no reflection* ($R_{ij}=0$) *much weaker than ideal transmission* $T_{ij}=\delta_{ij}$.

The evaluation of the various four-terminal resistances involves the chemical potentials on the upper and lower edges of the ideal leads, denoted by μ_{ul} , μ_{ll} , μ_{ur} , and μ_{lr} (see Fig. 8). By assumption, $\mu_{ul}=\mu_1$ and $\mu_{lr}=\mu_2$. Using the definitions of Büttiker *et al.*³⁰ one finds

$$\begin{aligned} \mu_{ll}-\mu_2 &= (\mu_1-\mu_2) \frac{\sum_i R_i/v_i}{\sum_i 1/v_i}, \\ \mu_{ur}-\mu_2 &= (\mu_1-\mu_2) \frac{\sum_i T_i/v_i}{\sum_i 1/v_i}. \end{aligned} \quad (13)$$

These forms agree with Eqs. (8) of SKM. We disregard for the moment questions related to the effects of strong coupling to the measurement reservoirs on voltage measurements, discussed by Büttiker.²⁹ Equation (13) applies in cases where the weak coupling to the measurement reservoir does not affect the system and where the measurement averages over the fluctuations on a scale of an electron wavelength. Thus, one obtains the four-terminal upper-edge resistance

$$R \equiv \frac{\mu_1-\mu_{ur}}{I} = \frac{h}{e^2} \frac{\sum_i R'_i/v_i}{\left[\sum_i 1/v_i\right] \sum_i T_i}, \quad (14)$$

and the Hall voltage measured on the LHS of the sample

$$R_H \equiv \frac{\mu_1-\mu_{ll}}{I} = \frac{h}{e^2} \frac{\sum_i T'_i/v_i}{\left[\sum_i 1/v_i\right] \sum_i T_i}. \quad (15)$$

Equations (14) and (15) differ by an index flip in the R_{ij} and T_{ij} in the numerator from Eqs. (10) and (9) of SKM. This slightly modifies the sum rule $G_0=(R+R_H)^{-1}$ [Eq. (11)] of SKM. The correct form follows from Eqs. (7) and (8):

$$G_0=(R'+R_H)^{-1}, \quad (16)$$

where R' , measured for $\mu_2 \geq \mu_1$, is given by

$$R' = \frac{h}{e^2} \frac{\sum_i R_i/v_i}{\left[\sum_i 1/v_i\right] \sum_i T_i}. \quad (17)$$

We remark that time-reversal symmetry guarantees $R(H)=R'(-H)$, but generally

$$R(H) \neq R'(H), \quad (18)$$

which is physically due to the difference in the scattering of electrons fed into the lower and upper edges of the sample. It would be interesting to observe this difference in a dc experiment.

What are the conditions for the QHE? A sufficient condition is T_i independent of i for all i [it can easily be checked by substituting this condition into Eq. (15) and using the identity $\sum_i T_i = \sum_i T'_i$]. Moreover, assuming that the T_i 's are monotonic functions of the velocities v_i (either increasing or decreasing in the weak sense), the above condition turns out to be a necessary one as well (see the discussion based on Chebychev's inequality in the Appendix). We find then that the condition $T_{ij}=\delta_{ij}$ advocated by SKM is certainly sufficient, but much stronger than our condition. Using Chebychev's inequality and assuming the T_i 's to be monotonic in the velocities, it is also possible to relate R_H to the general dependence of T_i on v_i . If the transmission is a monotonically increasing function of the velocity then $R_H \geq h/e^2 n$ while if it is a descending function $R_H \leq h/e^2 n$. Another possibility leading to QHE is v_i independent of i . This might occur (at least approximately) in the strong-field limit with small number of Landau levels.

A very interesting and plausible case is $R_{ij}=0$ (Ref. 29), which still allows an arbitrary scattering among upper or lower channels, but no mixing between these two sets. By Eqs. (1) and (2), this condition implies $R'_{ij}=0$, $T_i=1$, and $T'_i=1$, leading to

$$R'=R=0, \quad \frac{1}{R_H} = G_0 = n \frac{e^2}{h}. \quad (19)$$

Thus, the contact resistance quantization and the QHE are intimately related. When both hold, the chemical potential is constant along the upper (lower) edge and given by μ_1 (μ_2). Steps in the two-terminal conductance in a narrow strip at high fields have been observed by Wharam *et al.*³² and more recently by Kastner *et al.*³³

A curious result for the QHE follows from the above analogy. Defining the combined contact resistance $R_c=1/G_0-R$, it was found⁶ that it is equal to $h/e^2 n$ (n includes spin degeneracy) for ideal contacts, but it is not exactly quantized for contacts with nontrivial ($R_{ij} \neq 0$) scattering. However, the difference of $(R_c)^{-1}$ from exact quantization is due to the inverse velocity factors [such as in Eqs. (14)–(17)]. Exact quantization of $(R_c)^{-1}$ and $(R_H)^{-1}$ would follow if the v_i 's were equal or if the T_i 's were equal. In one particular case, that of a single channel,⁶ the velocity factor cancels and $R_c=h/e^2$ for arbitrary scattering. Thus, one is lead to the conclusion that when the Hall effect is due to surface states and when the field is strong enough (or E_F small enough) to have a single channel, the Hall conductance is quantized, $R_H=h/e^2$, up to rather strong disorder (actually up to a disorder of the order of $\hbar\omega_c$). This indeed follows trivially from Eq. (15) for an arbitrary scattering or longitudinal resistance. The system investigated in Secs. II–VI is another example for a single-channel Hall quantization with nonvanishing longitudinal resistance.

VIII. SUMMARY

We have investigated the magnetotransport due to edge states in a system smaller than the phase coherence length L_ϕ (for those states). For a strip topology it was shown that a sufficient condition for the QHE to hold is

T_i or v_i independent of i for all i . If the T_i 's are assumed to vary monotonically with v_i it was proven that the above condition is also a necessary one. Two special cases were considered.

(a) $R_{ij}=0$, leading to a vanishing four-terminal longitudinal resistance and quantized Hall resistance. This is a very plausible condition as long as the effective disorder is smaller than $\hbar\omega_c$.

(b) For a strong enough magnetic field or low Fermi energy, all electrons reside in the lowest Landau level. In that effectively single-channel case, $R_H = h/e^2$ independently of R_{11} .

Another geometry considered was that of a 2D quantum dot driven by two narrower leads. For a Fermi energy in the edge-states regime we have demonstrated AB oscillations in both longitudinal and Hall resistances with a period corresponding approximately to one ϕ_0 in the whole sample. The averaged Hall resistance was shown to be quantized in a wide range of longitudinal resistances (again, QHE with finite longitudinal resistance) in agreement with the single-channel case in SKM's formalism.

The "ring topology" responsible for the AB effect results from the existence of edge states and finite scattering from the upper to the lower edges in the connections of the leads to the "dot." This scattering is enhanced by the disorder, leading to a larger oscillation amplitude for increased disorder. The effective area for the flux shrinks with enhanced disorder, resulting in a longer period of oscillation as a function of \mathbf{B} . The AB oscillations found are extremely robust against disorder and it takes an effective disorder energy of the order of $\hbar\omega_c$ to smear them.

A possible experimental realization of these effects might consist of a high-quality, 2D EG GaAs disk, $\sim 1 \mu\text{m}$ in diameter, driven by two narrower leads at fields of a tesla or more. The temperature should be of the order of 100 mK to guarantee $k_B T < \hbar\omega_c L_H/L$ and a coherence length L_ϕ longer than L . Measurements of the Hall

conductance, we predict, will show AB periodic oscillations superimposed on the usual quantized plateaus. In addition to the predicted oscillations one expects sharp fluctuations, characteristic of the QHE in narrow wires.³⁴ The longitudinal resistance should be oscillatory as well, similar to the magnetoresistance of ordinary rings.

ACKNOWLEDGMENTS

The authors are grateful to M. V. Berry, Y. Aharonov, O. Entin-Wohlman, and Y. Gefen for instructive discussions. This research was supported by grants from the Israeli Academy of Sciences and Humanities (Jerusalem, Israel) and the Minerva Foundation (Munich, Federal Republic of Germany).

APPENDIX: THE CHEBYCHEV INEQUALITY (REF. 35)

Let $\{a_i\}$ and $\{b_i\}$ be two monotonic series such that

$$a_1 \leq a_2 \leq a_3 \leq \dots \leq a_n \quad \text{and} \quad b_1 \leq b_2 \leq \dots \leq b_n$$

or

$$a_1 \geq a_2 \geq a_3 \geq \dots \geq a_n \quad \text{and} \quad b_1 \geq b_2 \geq \dots \geq b_n.$$

Then

$$n \sum_i a_i b_i \geq \left[\sum_i a_i \right] \left[\sum_i b_i \right]$$

and equality holds if and only if either $a_1 = a_2 = \dots = a_n$ or $b_1 = b_2 = \dots = b_n$. If one of the series is a monotonically increasing one while the other series is a monotonically decreasing one, it trivially follows that

$$n \sum_i a_i b_i \leq \left[\sum_i a_i \right] \left[\sum_i b_i \right]$$

and equality holds if and only if either $a_1 = a_2 = \dots$ or $b_1 = b_2 = \dots = b_n$.

¹For an instructive discussion, see R. Peierls, *Surprises in Theoretical Physics* (Princeton University Press, Princeton, 1979), pp. 99–110.

²R. B. Dingle, Proc. R. Soc. (London) Ser. A **216**, 118 (1953); **219**, 463 (1953).

³M. Robnik, J. Phys. A **19**, 3619 (1986); M. V. Berry and M. Robnik, *ibid.* **19**, 649 (1986).

⁴T. W. Nee and R. E. Prange, Phys. Lett. A **25**, 582 (1967); R. E. Prange and T. W. Nee, Phys. Rev. B **168**, 779 (1968); M. S. Khaikin, Adv. Phys. **18**, 1 (1969).

⁵S. V. Iordanskii, Solid State Commun. **43**, (1982); S. A. Trugman, Phys. Rev. B **27**, 7539 (1983); R. F. Kazarinov and S. Luryi, *ibid.* **25**, 7626 (1982).

⁶See, e.g., Y. Imry, in *Directions in Condensed Matter Physics*, edited by G. Grinstein and G. Mazenko (World Scientific Singapore, 1986).

⁷E. N. Bogachev and G. A. Gogadze, Zh. Eksp. Theor. Fiz. **63**, 1839 (1972) [Sov. Phys.—JETP **36**, 973 (1973)].

⁸V. G. Peschanskii and V. V. Sinolitskii, Pis'ma Zh. Eksp. Theor. Fiz. **16**, 484 (1972) [JETP Lett. **16**, 344 (1972)].

⁹N. B. Brandt, D. V. Gitsu, A. A. Nikolaeva, and Ya. G. Ponomarev, Pis'ma Zh. Eksp. Theor. Fiz. **24**, 304 (1976) [JETP Lett. **24**, 272 (1976)]; Zh. Eksp. Theor. Fiz. **72**, 2332 (1977) [Sov. Phys.—JETP **45**, 1226 (1977)]; N. B. Brandt, E. N. Bogachev, D. V. Gitsu, G. A. Gogadze, I. O. Kulik, A. A. Nikolaeva, and Ya. G. Ponomarev, Fiz. Nizk. Temp. **8**, 718 (1982) [Sov. J. Temp. Phys. **8**, 358 (1982)].

¹⁰U. Sivan and Y. Imry, Phys. Rev. Lett. **61**, 1001 (1988).

¹¹B. I. Halperin, Phys. Rev. B **25**, 2185 (1982).

¹²P. Streda, J. Kucera and A. H. MacDonald, Phys. Rev. Lett. **59**, 1973 (1987).

¹³A. H. MacDonald and P. Streda, Phys. Rev. B **29**, 1616 (1984).

¹⁴M. Ya. Azbel, Solid State Commun. **54**, 127 (1985), and unpublished; M. Ya. Azbel and O. Entin-Wohlman, Phys. Rev. B **32**, 562 (1985).

¹⁵M. Büttiker, Y. Imry, and R. Landauer, Phys. Lett. A **96**, 365, (1983); R. Landauer and M. Büttiker, Phys. Rev. Lett. **54**, 2043 (1985); M. Büttiker, Phys. Rev. B **32**, 1846 (1985); Ann. N.Y. Acad. Sci. **480**, 194 (1986).

¹⁶O. Entin-Wohlman, C. Hartzstein, and Y. Imry; Phys. Rev. B

- 34, 921 (1986).
- ¹⁷R. Rammal, G. Toulouse, M. T. Jaekel, and B. I. Halperin, Phys. Rev. B **27**, 5142 (1983).
- ¹⁸D. R. Hofstadter, Phys. Rev. B **14**, 2239 (1976); M. Ya. Azbel, Zh. Eksp. Theor. Fiz. **46**, 929 (1964) [Sov. Phys.—JETP **19**, 634 (1964)]; M. Ya. Azbel, Phys. Rev. Lett. **43**, 1954 (1979).
- ¹⁹Y. Gefen, Y. Imry, and M. Ya. Azbel, Phys. Rev. Lett. **52**, 129 (1984); M. Büttiker, Y. Imry, and M. Ya. Azbel, Phys. Rev. A **30**, 1982 (1984).
- ²⁰R. A. Webb, S. Washburn, C. Umbach, and R. A. Laibowitz, Phys. Rev. Lett. **54**, 2696 (1985).
- ²¹M. Tsukada, J. Phys. Soc. Jpn. **41**, 1466 (1976).
- ²²M. Ya. Azbel and O. Entin-Wohlman, Phys. Rev. B **32**, 562 (1985); M. Ya. Azbel (unpublished).
- ²³R. Mehr and A. Aharony, Phys. Rev. B **37**, 6349 (1988).
- ²⁴J. K. Jain [Phys. Rev. Lett. **60**, 2074 (1988)] published a somewhat similar model for an ordinary ring without referring to previous, more general models (Ref. 19). However, the model presented here describes a *singly connected geometry* and does not allow for opposite currents in the arms. Jain does not obtain the oscillations of the Hall conductance around the quantized value.
- ²⁵H. L. Engquist and P. W. Anderson, Phys. Rev. B **24**, 1151 (1981).
- ²⁶U. Sivan and Y. Imry, Phys. Rev. B **33**, 551 (1986).
- ²⁷J. K. Jain and S. A. Kivelson, Phys. Rev. Lett. **60**, 1542 (1988).
- ²⁸G. Timp, H. U. Baranger, P. de Vegvar, G. E. Kunningham, R. E. Howard, R. Behringer, and P. M. Mankiewich, Phys. Rev. Lett. **60**, 2081 (1988).
- ²⁹M. Büttiker, Phys. Rev. B **38**, 9375 (1988).
- ³⁰M. Büttiker, Y. Imry, R. Landauer, and S. Pinhas, Phys. Rev. B **31**, 6207 (1985).
- ³¹B. J. Van Wees, H. van Houten, C. W. J. Beenakker, J. G. Williamson, L. P. Kouwenhoven, D. van der Marel, and C. T. Foxton, Phys. Rev. Lett. **60**, 848 (1988).
- ³²D. A. Wharam, T. J. Thornton, R. Newbury, M. Pepper, H. Ahmed, J. E. F. Frost, D. G. Hasko, D. C. Peacock, D. A. Ritchie, and G. A. C. Jones, J. Phys. C **21**, L209 (1988).
- ³³M. A. Kastner, S. B. Field, J. C. Licini, and S. L. Park, Phys. Rev. Lett. **60**, 2535 (1988).
- ³⁴M. L. Roukes, A. Scherer, S. J. Allen Jr., H. G. Craighead, R. M. Ruthen, E. D. Beebe, and J. P. Harbison, Phys. Rev. Lett. **59**, 3011 (1987).
- ³⁵*Tables of Integrals, Series, and Products*, edited by I. S. Gradshteyn and I. M. Ryzhik, corrected enlarged ed. (Academic, New York, 1980), p. 1094.